

# Direct (LC-)MS Identification of Regioisomers in C-H Activation by Partial Isotopic Labeling

Christopher A. Soj dak<sup>1</sup>, David A. Polefrone<sup>1</sup>, Hriday M. Shah<sup>1</sup>, Cassandra D. Vu<sup>1</sup>, Brandon J. Orzolek<sup>1</sup>, Pedro Jimenez Antenucci<sup>1</sup>, Micah Valadez Bush<sup>1</sup>, and Marisa C. Kozlowski<sup>1\*</sup>

5

<sup>1</sup>Department of Chemistry, University of Pennsylvania; Philadelphia, PA 19104, USA.

\*Corresponding author. Email: [marisa@sas.upenn.edu](mailto:marisa@sas.upenn.edu) (M. C. K)

10

15

20

**Abstract:** C–H functionalization of complex substrates is highly enabling in total synthesis and in the development of late-stage drug candidates. Much work has been dedicated towards developing new methods as well as developing predictive modeling to accelerate route scouting. However, workflows to identify regioisomeric products are arduous, typically requiring chromatographic separation and/or nuclear magnetic resonance spectroscopy analysis. In addition, most reports focus on major products or do not assign regioisomeric products which biases predictive models constructed from such data. Herein, we present a novel approach to complex reaction analysis utilizing partial deuterium labels which enables direct product identification via liquid chromatography–mass spectrometry. When combined with spectral deconvolution, the method generates product ratios while circumventing chromatography altogether. Competitive kinetic isotope effects can also be determined. The resultant data is expected to be useful in the construction of predictive models across several dimensions including reaction selectivity, the impact of structure on mechanism, and mass spectral ionization patterns.

25

**One-Sentence Summary:** The use of partial deuterium labels allows for direct identification of isomeric products in C-H activation without the need for separation.

## Main Text:

The use of late-stage functionalization (LSF) to alter the molecular properties of drug candidates late in development has become an essential part of modern medicinal chemistry and drug discovery. Optimizing the potency and pharmacokinetic characteristics of preexisting or drugs late in development represents a more cost-effective approach compared to initiating the development process anew with a novel compound. Of particular interest is C–H functionalization and to this end a large body of work now exists allowing for the functionalization of complex and structurally diverse compounds.<sup>(1-3)</sup>

Although incredible progress has been made in developing LSF, predicting outcomes when regioisomeric products are possible is often difficult. To this end, efforts have been devoted to developing predictive models. For example, in 2023 the Hartwig group developed a model which could predict the major reactive site of an iridium-catalyzed C–H borylation of six arenes.<sup>(4)</sup> The underlying data for such modeling relies on identifying the major product isomers in a large number of transformations. While high throughput experimentation is well-suited to rapidly conducting a large number of reactions to collect such data, identification of products when different isomers can form is challenging. Typically, such data is obtained by isolation of the relevant products and subsequent nuclear magnetic resonance (NMR) spectroscopic analysis. When more than one product is obtained, this workflow rapidly becomes more difficult as isomers are difficult to separate, and NMR analysis of multiple products is required (**Fig. 1A**). Once identities are secured, quantitation can be undertaken via liquid chromatography (LC) or gas chromatography (GC) coupled with UV-Vis or mass spectral (MS) detection typically with calibrated standards<sup>(5)</sup>; (**Fig. 1A**). While evaporative light scattering detection (ELSD) and charged aerosol detection (CAD) MS techniques can provide improved quantitation without separation or standards relative to matrix assisted laser desorption ionization (MALDI) or desorption electro-spray ionization (DESI), none of these approaches directly overcome the challenge of isomer identification.<sup>(6)</sup> The current methods for quantification of isomeric ratios are slow and/or cost prohibitive such as NMR in line with LC,<sup>(7)</sup> molecular rotational resonance spectroscopy (MRR),<sup>(8)</sup> ion mobility spectrometry–mass spectrometry (IMS–MS),<sup>(9)</sup> or niche in their application, such as DNA or peptide analysis via mass fragmentation.<sup>(10)</sup>

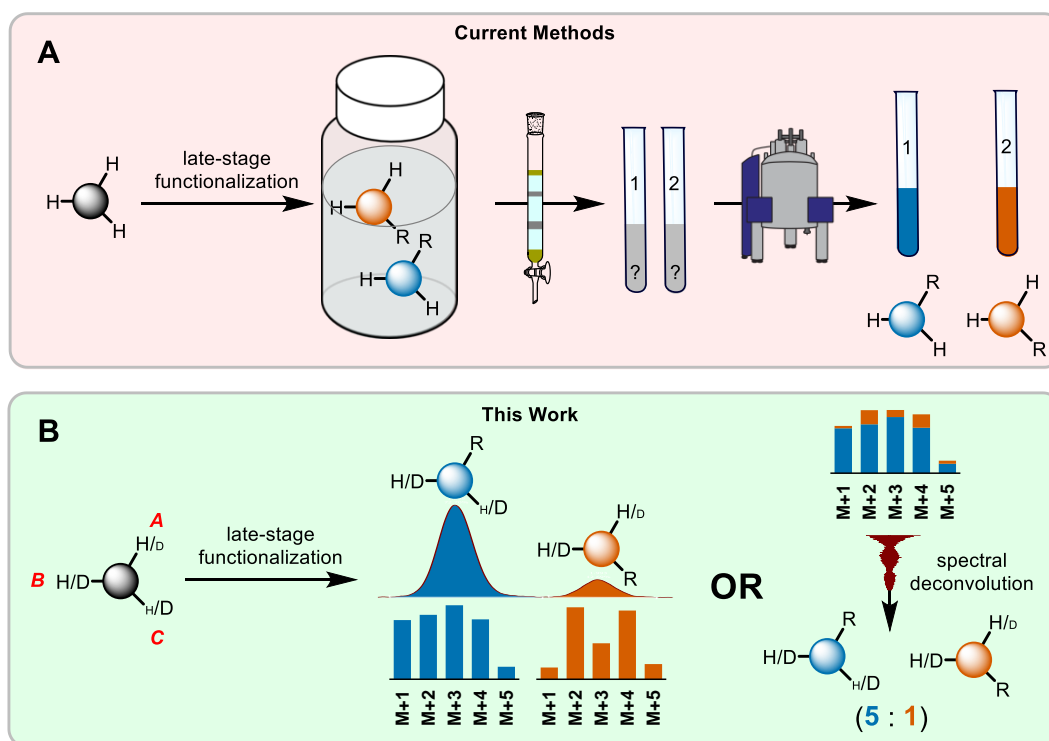


**Fig. 1.** A. Traditional workflow to identify mixtures of regioisomers. B. Our work using isotopic labels to identify separated and unseparated mixtures of regioisomers.

With the goal of rapidly generating data sets for machine learning to generate predictive models of C-H functionalization where regioisomeric outcomes are possible, we propose utilizing deuterium ( $^2\text{H}$  or D) as an isotopic label to identify regioisomers. Distinct partial isotopic labeling of reactive sites on a substrate, allows for the direct LC/MS identification of regioisomers and product ratios can even be successfully determined using spectral deconvolution to circumvent LC separation altogether (**Fig. 1B**).

### Method Development

To identify regioisomers via their unique isotopic distribution, potential reactive sites were labeled with differing amounts of deuterium. For example, a conventional C-H functionalization having three reactive sites A, B, and C with different amounts of deuterium at each position (A=25%  $^2\text{H}$ ; B=50%  $^2\text{H}$ ; C=75%  $^2\text{H}$ ) would lead to each unique product exhibiting a distinct isotopic fingerprint. In this case, the product from reaction occurring at position A forms a noticeably lighter product compared to that formed from reaction at position C. As a consequence, direct regioisomer identification can be accomplished by simple LC/MS analysis. The incorporation of deuterium into drugs has been used as a strategy to improve pharmacokinetic properties or reduce toxicity relative to their protio counterparts.<sup>(11)</sup> In addition, the greater use of analytical mass spectrometry has created a demand for internal deuterated standards and tritiated compounds are used in many aspects of drug discovery and development. Altogether, these needs have driven substantial development in undirected deuterium labeling of  $sp$ ,  $sp^2$ , and  $sp^3$  centered C-H

bonds, often utilizing D<sub>2</sub>O as an inexpensive deuterium source.(12-16) Leveraging these well-established methods allows for the rapid generation of the deuterated analogs needed for this approach with a broad range of molecules.

Minisci reactions of *N*-heterocycles are highly enabling in medicinal chemistry discovery.(17) However, multiple isomers can form as in the case of 3-substituted pyridines. Using a modified literature procedure, [D]-methyl nicotinate ([D]2) with different levels of deuterium labels at the C2, C4, C5, and C6 positions was generated by a straightforward palladium catalyzed exchange with D<sub>2</sub>O (18) followed by esterification (Fig. 2A). Labeled [D]2 was then subjected to conventional Minisci coupling conditions using *para*-tolylboronic acid as a radical source.(19) The unpurified reaction mixture was analyzed by LC/MS analysis and the experimental isotopic distributions (M+1 to M+5) of the LC product peaks (colored bars = experimental) were compared with the predicted values from the deuterium labels measured in the starting material (black bars) allowing assignment of the individual peaks *without isolation* (Fig. 2A). No C5 product was observed in line with prior literature.(19, 20) The identity of these products was later confirmed by isolating the individual peaks, securing the identify of each by <sup>1</sup>H NMR spectroscopy, and comparing LC retention times with the isolated standards (see Supplementary Information, SI).

Using the isotopic distributions (M+1–M+5) expected for each product obtained from the <sup>1</sup>H NMR of the starting material, ordinary least squares or non-negative least squares analysis allows the relative amount of each isomer to be deconvoluted without separating the isomers (Fig. 1B). Direct injection of the sample to the mass detector provides five unique m/z values (M+1–M+5) which can be expressed as a vector, P<sub>CR</sub>, and correlated to the weights of the three isomers (w<sub>2</sub>, w<sub>4</sub>, w<sub>6</sub>) expressed as vector w<sub>x</sub> (see SI for details). For the experiment from Fig. 2A, matrix deconvolution gives rise to similar product ratios compared to that from conventional LC UV-Vis analysis using calibrated standards (Fig. 2B).

### Parallel Microscale Reactions

With these promising results (Fig. 2A/B), six 3-substituted pyridines ([D]2–[D]7) were prepared from a common labeled intermediate [D]1 which simplifies introduction of the appropriate levels of labeling. A 24-well plate was designed for Minisci coupling on a 1 μmol scale of these six 3-substituted pyridines ([D]2–[D]7) with four electronically diverse aryl radicals (Fig. 2C). Each sample was analyzed by MS *without* separation in triplicate and product ratios were deconvoluted using isotopic distributions from the starting substrate (Fig. 2C). Importantly, with a run time of ~0.3 min for a loop injection vs a standard 5-min LC method, a 24-well plate can be analyzed in 7.2 min vs. 120 min which represents a 17-fold decrease in chromatography time.

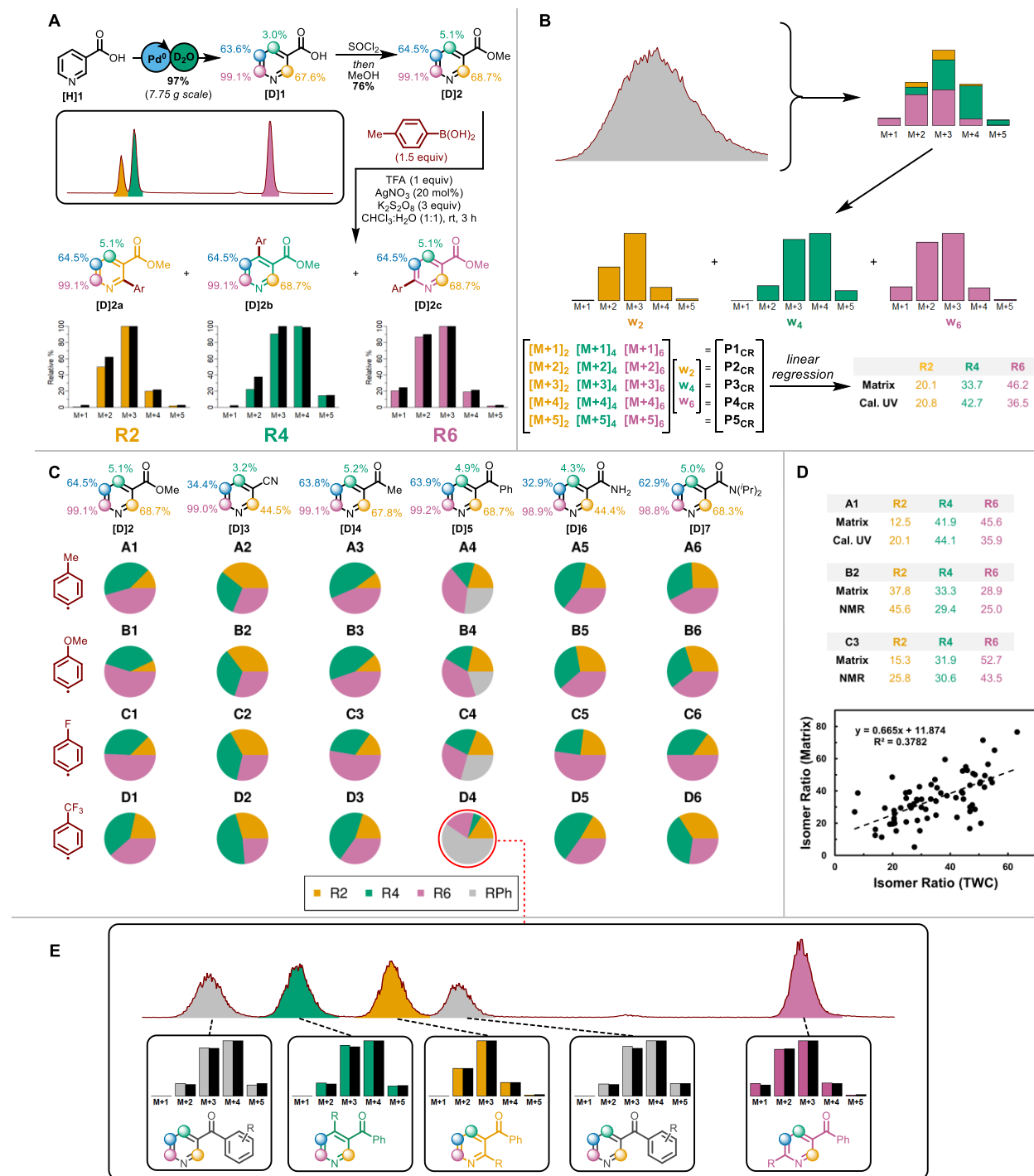


**Fig. 2.** **A.** Proof of concept. **B.** Matrix deconvolution of proof-of-concept reaction. **C.** 24-Well plate depicting Minisci coupling reactions between [D]2–[D]7 and four aryl radicals. Product ratios are determined via NNLS deconvolution. **D.** (top) Select examples comparing the matrix deconvoluted product ratios and product ratios from protio trial for wells: A1; B2; C3. (bottom) Comparison of matrix deconvolution results with total wavelength chromatogram (TWC) ratios. **E.** LC trace showcasing the isotopic patterns of the five products formed in well D4.

These data were compared to additional analysis of each sample by LC/MS where each product peak was identified solely on the basis of the MS isotopic labels and was quantified via uncalibrated UV-Vis (TWC). Notably, the isotopic labeling readily identified when the elution order was changed for the isomers in several cases including that shown in **Fig. 2E**. Additional product peaks were observed for the substrate **[D]5** arising from radical addition to the phenyl ring (labeled as RPh), and in the case of well D4 five unique products were identified from the isotopic distributions (**Fig. 2E**). Thus, it is best practice to incorporate reaction from an unlabeled site in the matrix deconvolution if it is possible for reaction to occur at other sites anywhere in the molecule. Uncalibrated TWC product ratios are currently the state-of-the-art for rapid analysis of isomeric product ratios, but do require LC separation and are subject to error if isomers have significantly different absorption values (1.7-1.9x measured in the case of well A1). Notably, the matrix method gives fair agreement relative to TWC values (**Fig. 2D**). While different ionization efficiencies of the isomers can cause errors in the matrix method, such differences are typically small, 1.2-1.5x measured in the case of well A1, as the isomers have similar molecular volumes and charge distributions.<sup>(21)</sup> On the basis of additional calibrated LC/UV or <sup>1</sup>H NMR spectroscopic analysis of larger scale reactions corresponding to wells A1, B2, and C3, the results from the matrix MS values are as good or better relative to the TWC values (**Fig. 2D**).

### Other sp<sup>2</sup> and sp<sup>3</sup> LSFs

To further establish the utility of the method, a variety of targets for LSF were selected including **[H]8-11** (**Fig. 3**). Isotopically labeled versions **[D]8-10** were readily synthesized via a reversible Pd<sup>II</sup> catalyzed C-H insertion in the presence of D<sub>2</sub>O.<sup>(22)</sup> In the case of **[D]10** an alternate, more sterically encumbering, ligand was needed to provide different levels of deuteration. **[D]11**, was obtained using a photocatalyzed HAT mediated deuteration.<sup>(23)</sup>

Bromination of etodolac and estrone derivatives **[D]8-9** was accomplished using *N*-bromosuccinimide (NBS).<sup>(24)</sup> The distinctive isotopic patterns easily allow the resultant products to be distinguished from one another (**Fig. 3A**). Moreover, deconvolution of unseparated materials exhibited excellent agreement with the calibrated UV-Vis ratios. Increasingly complex LSFs were performed on nateglinide derivative **[D]10** (**Fig. 3B**), and benzyl protected indoline **[D]11** (**Fig. 3C**). Palladium catalyzed C-H cyanation<sup>(25)</sup> of the sp<sup>2</sup> centers in **[D]10** resulted in the formation of three products **[D]10a-c**, with the LC peak for each being readily identified by their MS isotopic patterns. Furthermore, deconvolution of unseparated material led to excellent agreement with calibrated UV-VIS ratios, despite **[D]10** having less distinction between positions compared to **[D]2-7** (~12/16/39% vs. ~30/64/94%). The method was also effective with sp<sup>3</sup> centers. Specifically, photocatalytic arylation **[D]11**, via an  $\alpha$ -amino radical intermediate<sup>(26)</sup>, led to the formation of two products **[D]11a-b**, both of which were identified through their MS isotopic patterns.

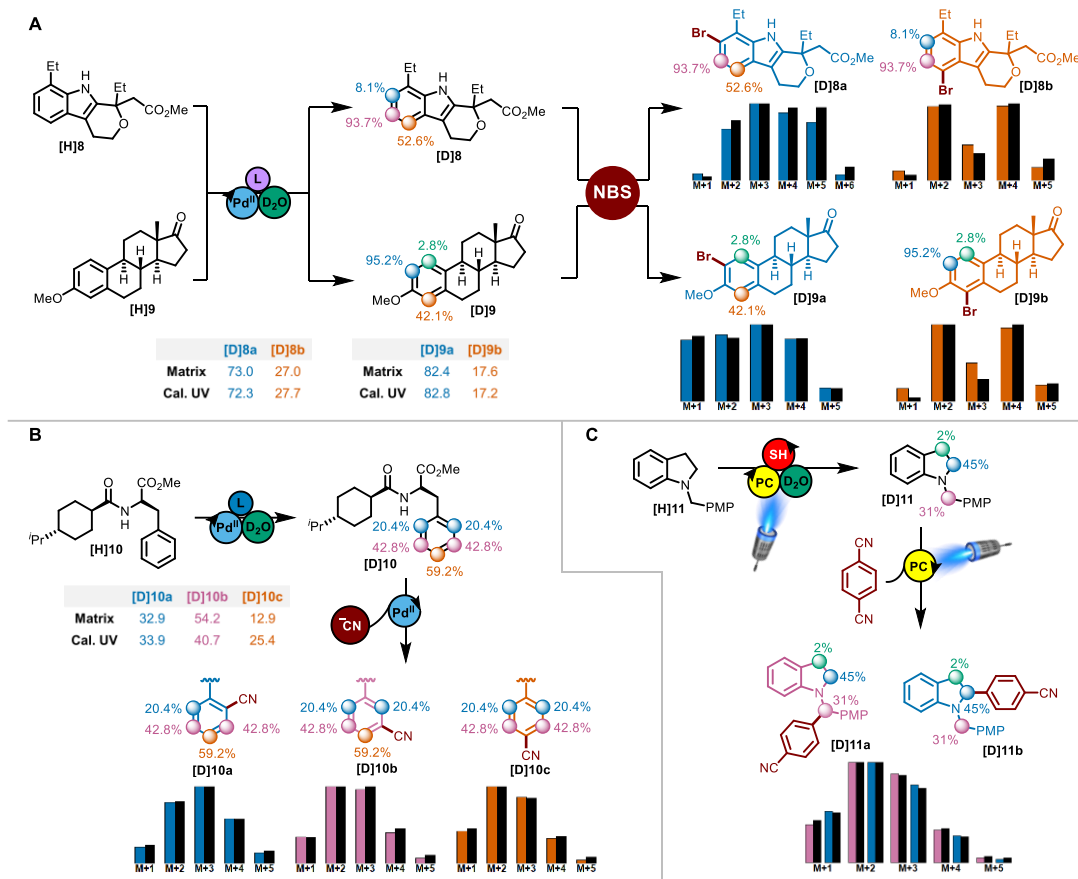


**Fig. 3. A.** NBS Bromination of [D]8-9. **B.** Pd<sup>II</sup> catalyzed cyanation of [D]10. **C.** Photocatalytic arylation of [D]11. In all figures, predicted isotope distributions are depicted in black while experimentally observed are represented as colored bars.

## 5 Kinetic Isotope Effects

When utilizing partially labeled materials, the product ratios from reactions exhibiting a KIE are not representative of those observed with protio material. As a result of the decreased rate observed at deuterated centers, positions with a greater degree of deuterium incorporation will be underrepresented in the final product ratio. Depending on the degree of accuracy required, this effect need not be considered in many systems (if competitive KIE  $\leq 3$ ) as the consequences of such isotope effects at low conversion are small (see SI).

However, this technique *can* also be used to both obtain the inherent product ratios of the protio substrates as well as the competitive KIE values providing an opportunity to collect mechanistic information in a high throughput manner. Determination of the presence of a KIE in these systems is easily determined if there is a change in the MS isotope pattern of residual starting material. By diluting the original deuterio substrate with pure protio substrate as shown in **Fig. 4A**, the effect of a KIE will diminish. As shown with the system of equations and graphically in **Fig. 4B**, the data can be extrapolated to identify

the regioselectivity ratio of the pure protio material (y-intercept, for  $[H]12a/[H]12b$ , this method = 2.10, standard from nondeuterated material = 2.16) and the slope can be used to determine the KIE value (this method = 1.78, standard competitive KIE method = 1.80). Similar analysis of multiple positions can also be done as in the case of pyridine  $[H/D]12''$  (Fig. 4C) and nateglinide derivative  $[D]10$  (Fig. 4D). This method is robust at determining product ratios, but care should be taken with competitive isotope effects (KIE <4) which can be sensitive to small changes in product ratios as was the case for Fig. 4D.

5

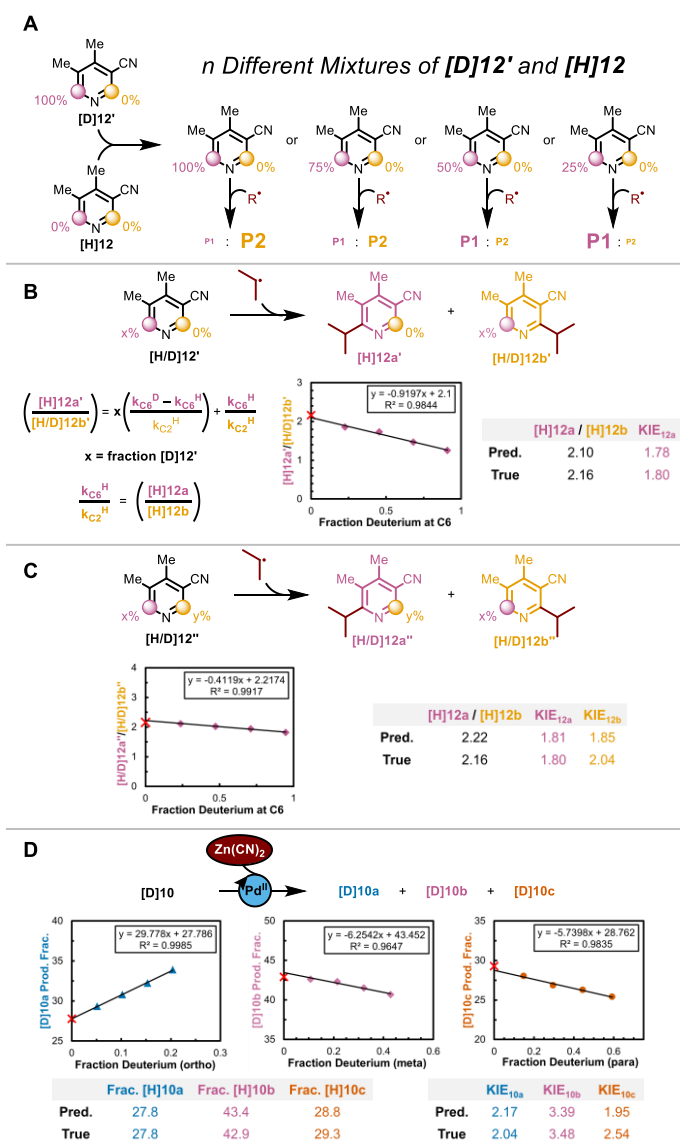


**Fig. 4.** **A.** Example of dilution experiments. **B.** Simplified model system with one position partially labeled. **C.** More complex model with two positions partially labeled. **D.** Analysis of cyanation of  $[D]10$ . In all plots the red X marks the experimentally obtained product fraction or ratio.

10



## Outlook

The novel mass spectral approach to reaction analysis utilizing partially isotopically labeled substrates developed herein allows direct identification of multiple regioisomers from C-H functionalization reactions in LC workflows and is effective with both  $sp^2$  and  $sp^3$  hybridized centers. Alternative methods for regioisomer identification require time consuming methods development, molecular modeling, lengthy acquisition times, the use of standards, or costly instrumentation. In contrast, this method can be implemented using conventional LC-MS methods with a range of detectors (single quadrupole and triple quadrupole) and rudimentary isotopic pattern calculations. Furthermore, the use of spectral deconvolution allows enumeration of regioisomeric ratios as well as relative reactivity without recourse to chromatographic separation enabling rapid analysis. This method sets the stage for collection of both larger and richer data sets containing information about minor isomers that are typically disregarded when a “major” product is isolated. In doing so, opportunities will abound to develop methods that target “minor” isomers selectively. Additionally, competitive KIE values can also be collected by dilution with unlabeled substrates allowing facile mechanistic interrogation of large portions of reaction space. The resultant data is expected to be useful in the construction of predictive models across several dimensions including predicting reaction selectivity, predicting mass spectral ionization efficiencies, and developing methods to identify isomers from mass spectral fragmentation patterns.(27)

**Acknowledgments: Funding:** We are grateful to the NIH (R35 GM131902) for financial support of this research. D. A. P. thanks the NSF GRFP fellowship (DGE-2236662). Partial instrumentation support was provided by the NIH (1S10OD011980, S10RR023444, 3R01GM118510-03S1, 3R01GM087605-06S1) and NSF (CHE-0848460, CHE-1827457) as well as the Vagelos Institute for Energy Science and Technology. **Author Contributions:** M.C.K., C. A. S., D. A. P., H. M. S., C. D. V., and P. J. A. designed the chemistry experiments. C. A. S., D. A. P., H. M. S., C. D. V., P. J. A., and M. V. B. performed the chemistry experiments. B. J. O., D. A. P., C. A. S., H. M. S., and C. D. V. developed the analytical methods. M.C.K., C. A. S., D. A. P., and H. M. S. performed the data analysis. M.C.K., C. A. S., and D. A. P. wrote the manuscript. **Competing Interests:** None Declared **Data and materials availability:** All data described in this work are included in the supplementary materials.

## Supplementary Materials:

Materials and Methods

Figures S1 to S279

Tables S1 to S30

References

## References and Notes:

1. N. J. Castellino, A. P. Montgomery, J. J. Danon, M. Kassiou, Late-stage Functionalization for Improving Drug-like Molecular Properties. *Chem. Rev.* **123**, 8127-8153 (2023).
- 5 2. L. Guillemard, N. Kaplaneris, L. Ackermann, M. J. Johansson, Late-stage C–H functionalization offers new opportunities in drug discovery. *Nature Reviews Chemistry* **5**, 522-545 (2021).
3. L. Zhang, T. Ritter, A Perspective on Late-Stage Aromatic C–H Bond Functionalization. *J. Am. Chem. Soc.* **144**, 2399-2414 (2022).
- 10 4. E. Caldeweyher *et al.*, Hybrid Machine Learning Approach to Predict the Site Selectivity of Iridium-Catalyzed Arene Borylation. *J. Am. Chem. Soc.* **145**, 17367-17376 (2023).
5. M. A. McDonald, B. A. Koscher, R. B. Canty, K. F. Jensen, Calibration-free reaction yield quantification by HPLC with a machine-learning model of extinction coefficients. *Chemical Science* **15**, 10092-10100 (2024).
- 15 6. V. V. Sharma, I. Lanekoff, Revealing Structure and Localization of Steroid Regioisomers through Predictive Fragmentation Patterns in Mass Spectrometry Imaging. *Anal. Chem.* **95**, 17843-17850 (2023).
7. T. Gebretsadik, W. Linert, M. Thomas, T. Berhanu, R. Frew, LC–NMR for Natural Product Analysis: A Journey from an Academic Curiosity to a Robust Analytical Tool. *Sci.* 2021 (10.3390/sci3010006).
- 20 8. Y. Song, Q. Song, W. Liu, J. Li, P. Tu, High-confidence structural identification of metabolites relying on tandem mass spectrometry through isomeric identification: A tutorial. *TrAC, Trends Anal. Chem.* **160**, 116982 (2023).
9. C. Laphorn, F. Pullen, B. Z. Chowdhry, Ion mobility spectrometry-mass spectrometry (IMS-MS) of small molecules: Separating and assigning structures to ions. *Mass Spectrom. Rev.* **32**, 43-71 (2013).
- 25 10. M.-Q. Liu *et al.*, pGlyco 2.0 enables precision N-glycoproteomics with comprehensive quality control and one-step mass spectrometry for intact glycopeptide identification. *Nature Communications* **8**, 438 (2017).
- 30 11. R. M. C. Di Martino, B. D. Maxwell, T. Pirali, Deuterium in drug discovery: progress, opportunities and challenges. *Nature Reviews Drug Discovery* **22**, 562-584 (2023).
12. S. Kopf *et al.*, Recent Developments for the Deuterium and Tritium Labeling of Organic Molecules. *Chem. Rev.* **122**, 6634-6718 (2022).
13. J. Atzrodt, V. Derdau, T. Fey, J. Zimmermann, The Renaissance of H/D Exchange. *Angew. Chem. Int. Ed.* **46**, 7744-7765 (2007).
- 35 14. J. Atzrodt, V. Derdau, W. J. Kerr, M. Reid, C–H Functionalisation for Hydrogen Isotope Exchange. *Angew. Chem. Int. Ed.* **57**, 3022-3047 (2018).
15. Q.-K. Kang, H. Shi, Catalytic Hydrogen Isotope Exchange Reactions in Late-Stage Functionalization. *Synlett* **33**, 329-338 (2021).
- 40 16. R. Zhou, L. Ma, X. Yang, J. Cao, Recent advances in visible-light photocatalytic deuteration reactions. *Organic Chemistry Frontiers* **8**, 426-444 (2021).
17. M. A. J. Dunston, Minisci reactions: Versatile CH-functionalizations for medicinal chemists. *MedChemComm* **2**, 1135-1161 (2011).
18. H. Esaki *et al.*, General method of obtaining deuterium-labeled heterocyclic compounds using neutral D<sub>2</sub>O with heterogeneous Pd/C. *Tetrahedron* **62**, 10954-10961 (2006).
- 45 19. I. B. Seiple *et al.*, Direct C–H Arylation of Electron-Deficient Heterocycles with Arylboronic Acids. *J. Am. Chem. Soc.* **132**, 13194-13196 (2010).

20. F. Minisci *et al.*, Polar effects in free-radical reactions. Solvent and isotope effects and effects of base catalysis on the regio- and chemoselectivity of the substitution of protonated heteroaromatic bases by nucleophilic carbon-centered radicals. *J. Org. Chem.* **52**, 730-736 (1987).
- 5 21. M. Oss, A. Krueve, K. Herodes, I. Leito, Electrospray Ionization Efficiency Scale of Organic Compounds. *Anal. Chem.* **82**, 2865-2872 (2010).
22. M. Farizyan, A. Mondal, S. Mal, F. Deufel, M. van Gemmeren, Palladium-Catalyzed Nondirected Late-Stage C–H Deuteration of Arenes. *J. Am. Chem. Soc.* **143**, 16370-16376 (2021).
- 10 23. Y. Y. Loh *et al.*, Photoredox-catalyzed deuteration and tritiation of pharmaceutical compounds. *Science* **358**, 1182-1187 (2017).
24. M. R. Rose, K. P. Reber, Kinetic Isotope Effects in Electrophilic Aromatic Halogenation of Dimethenamid in Chlor(am)inated Water Demonstrate Unique Aspects of Iodination. *Environmental Science & Technology Letters* **7**, 721-726 (2020).
- 15 25. H. Chen, A. Mondal, P. Wedi, M. van Gemmeren, Dual Ligand-Enabled Nondirected C–H Cyanation of Arenes. *ACS Catalysis* **9**, 1979-1984 (2019).
26. A. McNally, C. K. Prier, D. W. C. MacMillan, Discovery of an  $\alpha$ -Amino C–H Arylation Reaction Using the Strategy of Accelerated Serendipity. *Science* **334**, 1114-1117 (2011).
27. T. Vehovec, A. Obreza, Review of operating principle and applications of the charged aerosol detector. *J. Chromatogr. A* **1217**, 1549-1556 (2010).
- 20 28. M. Loos, C. Gerber, F. Corona, J. Hollender, H. Singer, Accelerated Isotope Fine Structure Calculation Using Pruned Transition Trees. *Anal. Chem.* **87**, 5738-5744 (2015).
29. M. Turowski *et al.*, Deuterium Isotope Effects on Hydrophobic Interactions: The Importance of Dispersion Interactions in the Hydrophobic Phase. *J. Am. Chem. Soc.* **125**, 13836-13849 (2003).
- 25 30. L. Martens *et al.*, mzML—a Community Standard for Mass Spectrometry Data\*. *Molecular & Cellular Proteomics* **10**, R110.000133 (2011).
31. M. C. Chambers *et al.*, A cross-platform toolkit for mass spectrometry and proteomics. *Nat. Biotechnol.* **30**, 918-920 (2012).
- 30 32. D. Kessner, M. Chambers, R. Burke, D. Agus, P. Mallick, ProteoWizard: open source software for rapid proteomics tools development. *Bioinformatics* **24**, 2534-2536 (2008).
33. DOI: 10.18129/B9.bioc.mzR.
34. DOI: 10.18129/B9.bioc.msdata
- 35 35. L. Gatto, K. S. Lilley, MSnbase—an R/Bioconductor package for isobaric tagged mass spectrometry data visualization, processing and quantitation. *Bioinformatics* **28**, 288-289 (2012).
36. C. C. Gruber *et al.*, An Algorithm for the Deconvolution of Mass Spectroscopic Patterns in Isotope Labeling Studies. Evaluation for the Hydrogen–Deuterium Exchange Reaction in Ketones. *J. Org. Chem.* **72**, 5778-5783 (2007).
- 40 37. <http://biocatalysis.uni-graz.at/pdf/IsoPat2.zip>.
38. A. P. Tulloch, Deuterium isotope effects and assignment of  $^{13}\text{C}$  chemical shifts in spectra of methyl octadecanoate and the sixteen isomeric oxooctadecanoates. *Can. J. Chem.* **55**, 1135-1142 (1977).
- 45 39. P. E. Hansen, F. S. Kamounah, D. T. Gryko, Deuterium Isotope Effects on  $^{13}\text{C}$ -NMR Chemical Shifts of 10-Hydroxybenzo[h]quinolines. *Molecules*. 2013 (10.3390/molecules18044544).

40. T. A. Darwish, N. R. Yepuri, P. J. Holden, M. James, Quantitative analysis of deuterium using the isotopic effect on quaternary <sup>13</sup>C NMR chemical shifts. *Anal. Chim. Acta* **927**, 89-98 (2016).
- 5 41. S. Pal *et al.*, Extract and fraction of *Cassia occidentalis* L. (a synonym of *Senna occidentalis*) have osteogenic effect and prevent glucocorticoid-induced osteopenia. *J. Ethnopharmacol.* **235**, 8-18 (2019).
42. T. Kawabata, H. Matsubara, Safe and facile evolution of diazomethane using the phase-vanishing method. *Tetrahedron Lett.* **123**, 154554 (2023).
- 10 43. K. K. Chouhan, D. Chowdhury, A. Mukherjee, Cyclotrimetaphosphate-assisted ruthenium catalyst for the hydration of nitriles and oxidation of primary amines to amides under aerobic conditions in water. *Organic & Biomolecular Chemistry* **21**, 2429-2439 (2023).
44. T. D. Weinhold *et al.*, Assessing Carbazole Derivatives as Single-Electron Photoreductants. *J. Org. Chem.* **87**, 16928-16936 (2022).
- 15 45. L. O'Brien, S. P. Argent, K. Ermanis, H. W. Lam, Gold(I)-Catalyzed Nucleophilic Allylation of Azinium Ions with Allylboronates. *Angew. Chem. Int. Ed.* **61**, e202202305 (2022).
46. A. Joshi, S. Kumari, S. Kundu, Photoredox (NN)Mn(I) Catalysed Acceptorless Dehydrogenation: Synthesis of Amides, Aldehydes and Ketones. *Adv. Synth. Catal.* **364**, 4371-4383 (2022).
- 20 47. H. Wu, A. Sumita, Y. Otani, T. Ohwada, Friedel–Crafts Acylation of Aminocarboxylic Acids in Strong Brønsted Acid Promoted by Lewis Base P4O10. *J. Org. Chem.* **87**, 15224-15249 (2022).
- 25 48. D. J. Robinson, K. G. Ortiz, N. P. O'Hare, R. R. Karimov, Dearomatization of Heteroarene Salts with ArBpin Reagents. Application to the Total Synthesis of a Nuphar Alkaloid. *Org. Lett.* **24**, 3445-3449 (2022).
49. K. M. Korch *et al.*, Selected Ion Monitoring Using Low-Cost Mass Spectrum Detectors Provides a Rapid, General, and Accurate Method for Enantiomeric Excess Determination in High-Throughput Experimentation. *ACS Catalysis* **12**, 6737-6745 (2022).
- 30 50. D. Zhao, P. Xu, T. Ritter, Palladium-Catalyzed Late-Stage Direct Arene Cyanation. *Chem* **5**, 97-107 (2019).
51. N. Fleury-Brégeot, J. Raushel, D. L. Sandrock, S. D. Dreher, G. A. Molander, Rapid and Efficient Access to Secondary Arylmethylamines. *Chem. Eur. J.* **18**, 9564-9570 (2012).
- 35 52. J. K. CLAUSEN Dane James; FELLS, Joseph; LIU, Ping; MAZZOLA, Robert, AZABICYCLO[4.1.0]HEPTANE ALLOSTERIC MODULATORS OF THE M4 MUSCARINIC ACETYLCHOLINE RECEPTOR, US2018035772W, (2018).